

1
2
3
4
5
6
7
8
9
10
11
12
13
14
15
16
17
18
19
20
21
22
23
24
25
26
27
28
29
30
31
32
33
34
35
36
37
38
39
40
41

Supplementary Information for

**Solar Power Ramps in the Future: Assessing Australia's Potential with
Climate Projections**

Shukla Poddar^{1,2}, Jason P Evans^{2,3}, Merlinde Kay¹, Abhnil Prasad^{1,2,3}, Stephen Bremner¹

¹School of Photovoltaic and Renewable Energy Engineering, University of New South Wales,
Sydney, Australia

²ARC Centre of Excellence for Climate Extremes, University of New South Wales, Sydney,
Australia

³Climate Change Research Centre, Biological, Earth and Environmental Sciences, University
of New South Wales, Sydney, Australia

Corresponding author: Shukla Poddar (s.poddar@unsw.edu.au)

42 **Contents of this file:**

43 1. Table 1s-6s

44 2. Figures 1s to 22s

45

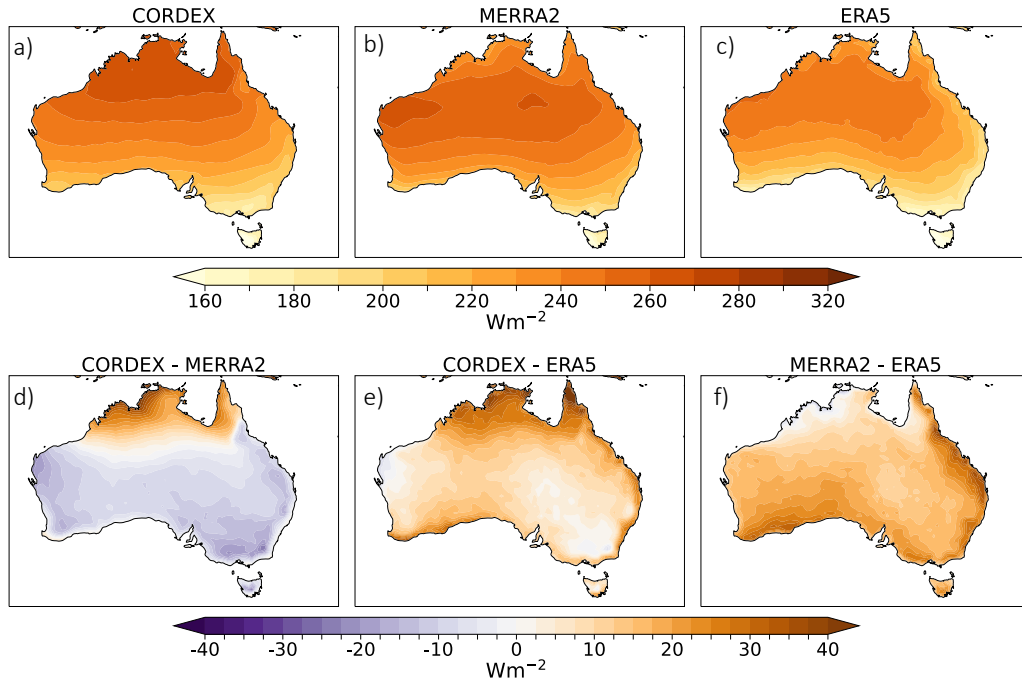
46 **Introduction**

47 This supporting information includes:

- 48 • Validation of CORDEX-Australasia ensemble mean radiation with two reanalysis products:
49 MERRA2 and ERA5 (**Figure 1s**).
- 50 • Details of PV technologies and modelling steps for simulating power with PVLIB (**Figure 2s,**
51 **Table 1s**).
- 52 • Evaluation of PVLIB model selection parameters (**Figure 3s, Table 2s-4s**).
- 53 • Validation of PVLIB power simulations with observations from DKASC solar farm (**Figure**
54 **4s, Table 5s**).
- 55 • CORDEX-Australasia RCM-GCM pairs used in the study (**Table 6s**).
- 56 • Mean power projections for from mono-crystalline silicon cells and future changes for various
57 ensemble members under RCP4.5 and RCP8.5 scenario (**Figure 5s-7s**).
- 58 • Ramp characteristics for the near future period (**Figure 8s-10s**).
- 59 • Future changes in mean solar ramp magnitude across Australia for the near future and far future
60 periods under RCP8.5 and RCP 4.5 scenario for the various ensemble members of CORDEX-
61 Australasia (**Figure 11s-12s**).
- 62 • Future changes in extreme solar ramp magnitude across Australia for the near future and far
63 future periods under RCP8.5 and RCP 4.5 scenario for the various ensemble members of
64 CORDEX-Australasia (**Figure 13s-14s**).
- 65 • Future changes in mean solar ramp frequency across Australia for the near future and far future
66 periods under RCP8.5 and RCP 4.5 scenario for the various ensemble members of CORDEX-
67 Australasia (**Figure 15s-16s**).
- 68 • Future changes in extreme solar ramp frequency across Australia for the near future and far
69 future periods under RCP8.5 and RCP 4.5 scenario for the various ensemble members of
70 CORDEX-Australasia (**Figure 17s-18s**).
- 71 • Future changes in mean solar ramping periods across Australia for the near future and far future
72 periods under RCP8.5 and RCP 4.5 scenario for the various ensemble members of CORDEX-
73 Australasia (**Figure 19s-20s**).
- 74 • Future changes in extreme solar ramp duration across Australia for the near future and far future
75 periods under RCP8.5 and RCP 4.5 scenario for the various ensemble members of CORDEX-
76 Australasia (**Figure 21s-22s**).

77
78
79
80
81
82

1. Validation of solar radiation from CORDEX-Australasia with reanalysis



83
84

85 **Figure 1s.** Validation of mean solar radiation of CORDEX-Australasia with two reanalysis products:
86 MERRA2 and ERA5. Panel a-c represents the mean solar radiation from 1980-2005 for a) CORDEX-
87 Australasia ensemble mean, b) MERRA2 c) ERA5. Panel d and e represent the mean bias error
88 ensemble mean of the CORDEX-Australasia simulations when compared with MERRA2 and ERA5,
89 respectively, for the historical period (1980-2005). Panel f) represents the difference in mean
90 downward shortwave radiation in MERRA2 and ERA5 for the historical period (1980-2005).

91

92 In this study, the ensemble mean of shortwave downwelling radiation has been evaluated using
93 two reanalysis products: Modern-Era Retrospective analysis for Research and Applications
94 Version 2 (MERRA2) and European Centre for Medium Range Weather Forecasts (ECMWF)
95 Re-analysis (ERA5), the historical period (1980-2005). We observe a positive bias near
96 Northern Australia in comparison with MERRA2 while negative biases rest of Australia. While
97 there is a similar positive bias in the Northern Australian region in comparison with ERA5 data
98 with negligible positive bias all over the continent. Overall, the CORDEX data captures the
99 solar radiation with reasonable fidelity over Australia, often falling between the two reanalysis.
100 These small differences in the CORDEX-Australasia radiation with the reanalysis products are
101 within an acceptable range. They can be mainly attributed to the sub-grid scale processes

102 occurring in the actual environment and the specific parameterization schemes selected to
 103 obtain the model simulations. This concise evaluation of the surface reaching downwards
 104 shortwave radiation in the CORDEX-Australasia ensemble and the previous evaluation studies
 105 on CORDEX-Australasia ensembles adds confidence to the results presented in the paper.

106
107

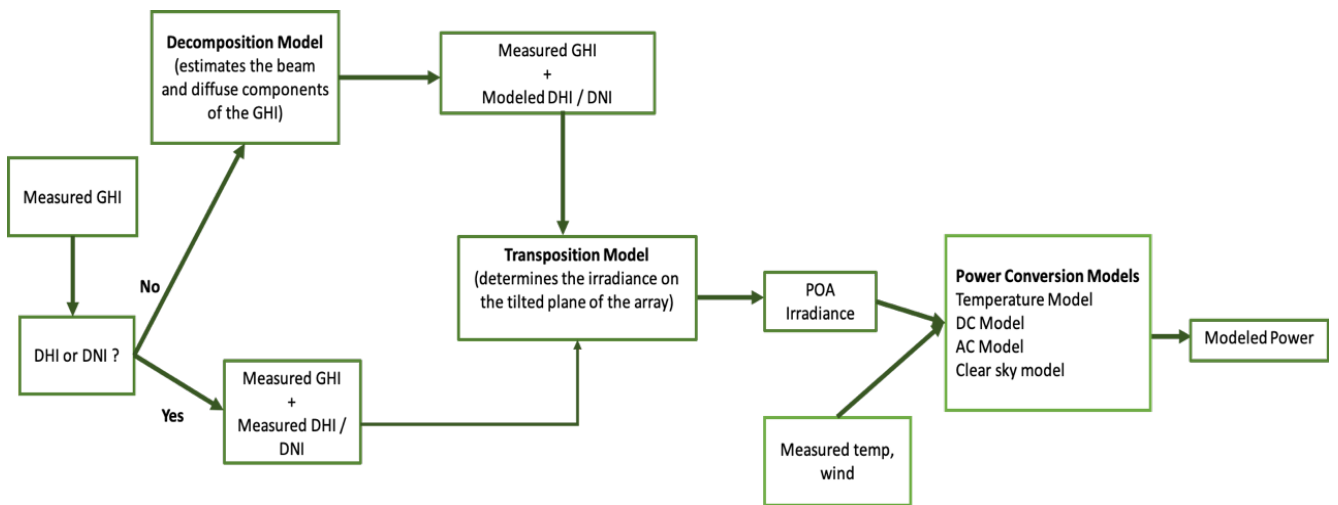
108 2. Details of PV technologies and modelling steps for simulating power with PVLIB

109
110

Table 1s. Details of the PV technology used for simulating and validating PV power using PVLIB

	Mono-Si	Multi-Si	CdTe
Panel Type	BP-Solar 4170N	Kyocera KD135GX-LP	First Solar FS 272
Inverter Type	SMA SMC 6000A	SMA SMC 5000A	Fronius Primo 6.0-1
Array Structure	Fixed	Fixed	Fixed
Array Tilt/Azimuth	20/0	20/0	20/0
Simulation Period	2010-2016	2010-2013	2010-2016

111
112
113



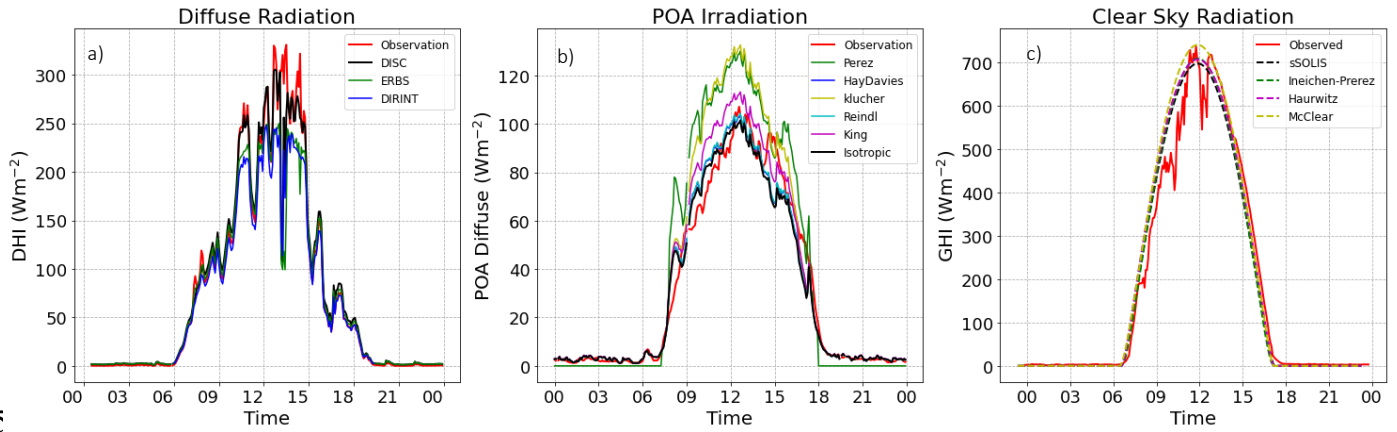
114
115
116

Figure 2s. Flowchart showing the various modelling steps in PVLIB.

117
118
119
120
121
122
123
124
125
126
127

128
 129
 130
 131
 132
 133
 134

3. Model Selection for PVLIB power simulations



135
 136
 137
 138
 139
 140
 141
 142
 143
 144

Figure 3s. Sample DHI, POA diffuse and clear sky radiation at every 5-minute interval from observations and modelled output obtained using PVLIB. Panel a), b) and c) represents the diurnal curves for DHI, POA diffuse irradiation and clear sky irradiation. The red line represents the observations recorded during the day.

Table 2s. Error metrics comparing diffuse horizontal irradiance (DHI) obtained from decomposition models with the DHI observations recorded at the weather station at DKASC solar farm

Decomposition Models	MBE (W/m ²)	RMSE (W/m ²)
Disc	10.550885	44.411851
ERBS	12.241542	45.937148
DIRINT	13.694237	52.020097

145
 146
 147
 148

Table 3s. Error metrics comparing plane of array (POA) DHI obtained from transposition models with the POA-DHI observations from the weather station at DKASC solar farm.

Transposition Models	MBE (W/m ²)	RMSE (W/m ²)
Isotropic	6.01	43.20
Hay Davies	6.32	44.27
Perez	11.64	47.96
klucher	12.31	46.32

Reindl	6.53	44.35
King	9.517	45.40

149
150
151
152
153
154
155

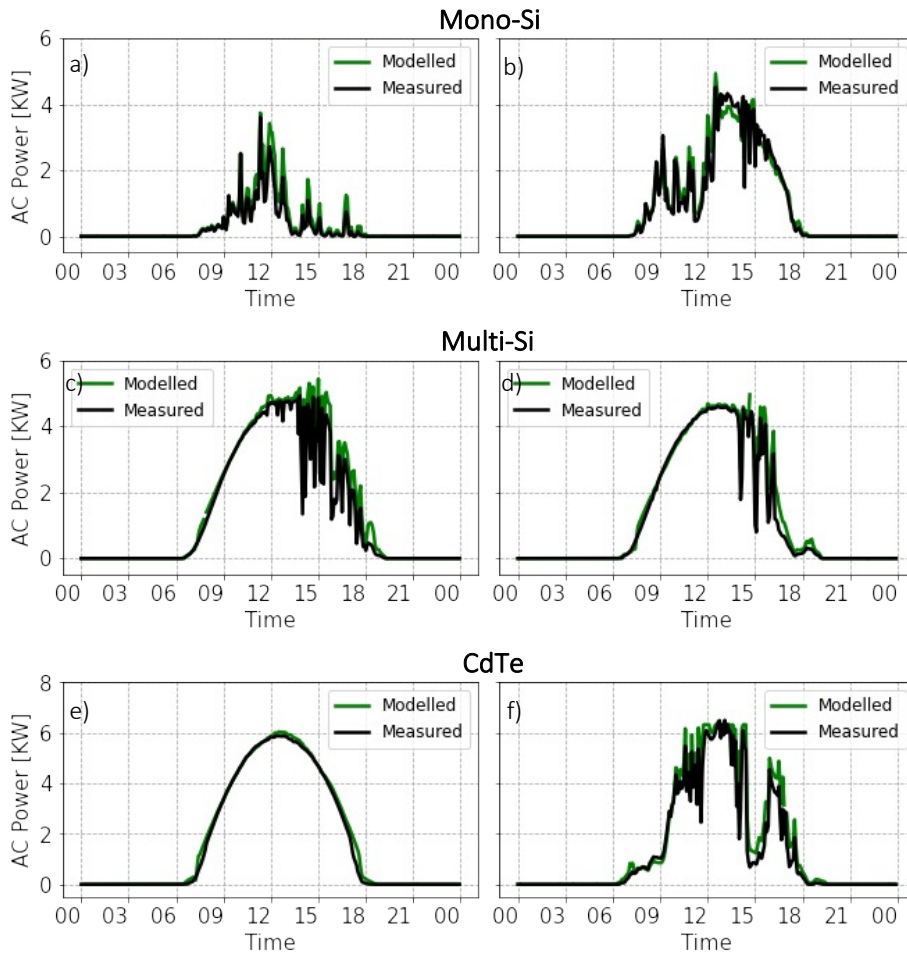
Table 4s. Error metrics comparing clear-sky global horizontal irradiation (GHI) obtained from clear-sky models with the clear-sky GHI from reanalysis product- MERRA2. The modelled GHI is compared with the station observations at DKASC solar farm by extracting GHI during the clear sky periods. The clear-sky periods are calculated following Reno [1].

Model	MERRA2		Observations	
	RMSE (W/m ²)	Mean Bias (W/m ²)	RMSE (W/m ²)	Mean Bias (W/m ²)
sSOLIS	23.056	0.914	19.825	-5.229
Inchein-Perez	26.112	-3.916	21.598	-6.172
Haurwitz	31.354	-5.090	28.329	-8.365
McClear	31.15	8.839	22.396	-1.308

156
157
158
159
160
161
162
163
164
165
166
167
168
169
170
171
172
173
174
175
176
177
178
179

180
181
182

4. Validation of PVLIB power simulations with observations from DKASC solar farm



183
184
185
186
187
188
189

Figure 4s. Sample PV power output at every 5-minute interval for different PV technologies obtained using PVLIB. Panel a) and b) represent the diurnal power curves for mono-crystalline Silicon cells. Panel c) and d) represent the diurnal power curves for multi-crystalline Silicon cells. Panel e) and f) represent the diurnal curve for thin film Cadmium Telluride cells. The black line represents the AC power output values recorded during the day. The green line represents the modelled AC power using PVLIB.

190
191
192

Table 5s. Error metrics comparing power projections obtained from PVLIB simulations and observations recorded at the DKASC solar farm recorded at every 5-minute.

PV Technology	Mean Bias (KW)	RMSE (KW)
Mo-Si	0.02	0.31
Mu-Si	0.06	0.39
CdTe	0.10	0.54

193

194
195
196
197
198

5. CORDEX-Australasia RCM-GCM pairs used in the study

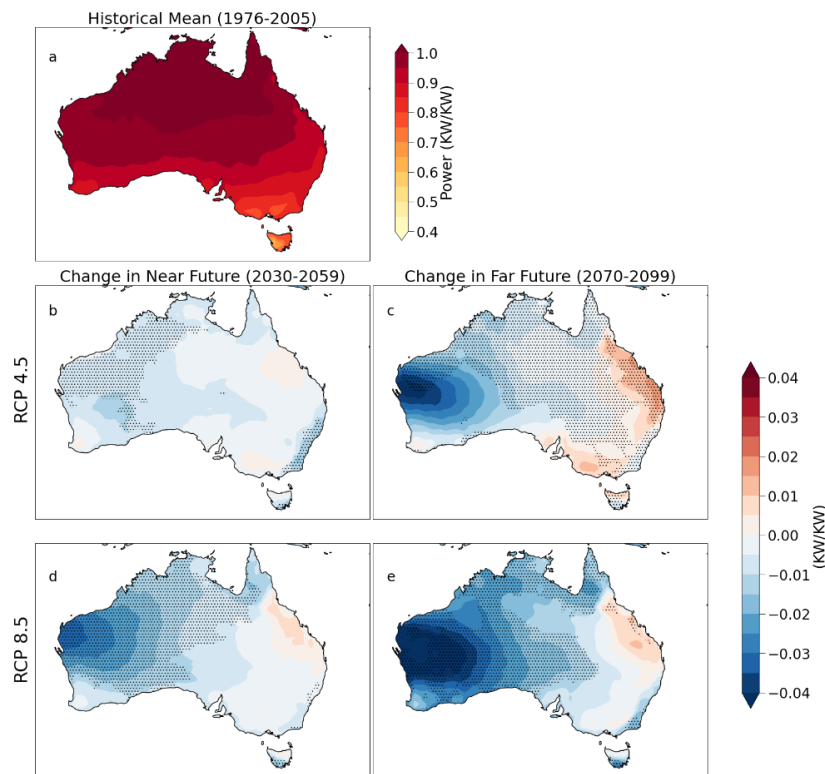
Table 6s. CORDEX-Australasia GCM-RCM pairs analyzed in this study provided climate projections for both the historical and future periods under RCP8.5 and RCP4.5 scenarios.

RCM GCM	WRF J	WRF K
ACCESS1.0		
ACCESS1.3		
CanESM2		

199
200

6. Mean power projections for Mo-Si cells and future changes for each ensemble member under RCP4.5 and RCP8.5 scenario

201
202
203
204

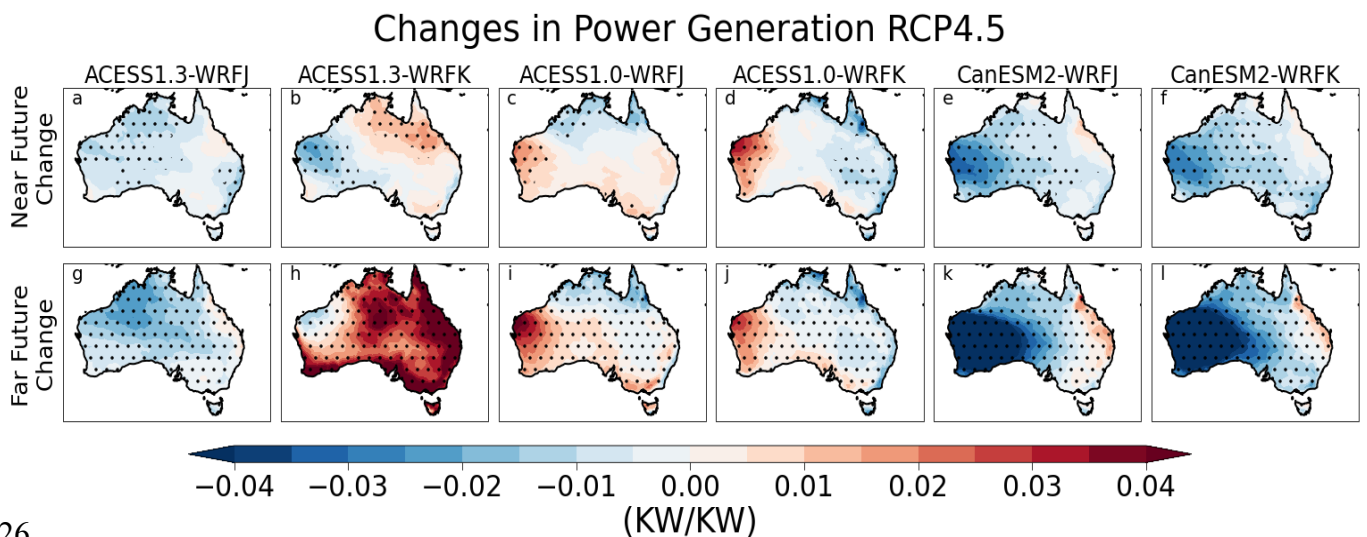


205
206
207
208
209
210
211

Figure 5s. Normalized PV Power across Australia. Panel a) represents the mean normalized power for the historical period (1976-2005). Panel b) and d) represent the future changes in the mean power for the near future (2030-2059) period under RCP4.5 and RCP8.5. Panel c) and e) represents the future changes in the mean power for the far future (2070-2099) period under RCP4.5 and RCP8.5. Stippling indicates a significant change (according to methods: significant test).

212
213
214
215
216
217
218
219
220
221
222
223
224
225

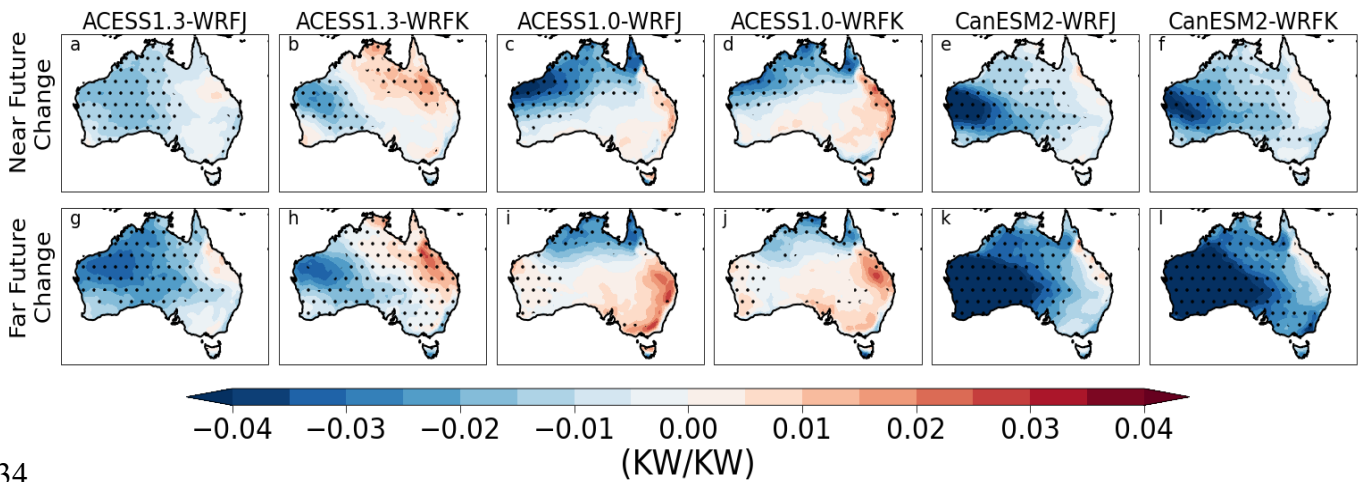
The mean normalized power generation capacity for the monocrystalline Silicon module during the historical period is shown in figure 4s a, and future changes under RCP4.5 and RCP8.5 scenarios are shown in figures 4s b - d for future periods. Due to high solar exposure at those locations, the historical power generation capacity is highest for Northern and Central Australia. During the near future, there is expected to be a slight decline in the power projection throughout the continent, with minor increases in eastern Queensland under both scenarios. There is a significantly higher decrease in the west under RCP8.5 during the near future, unlike RCP4.5. This decline intensifies in magnitude during the far future period for both scenarios. However, it is projected that the East and Southern coastal parts will undergo a small but significant increase in power generation capacity during the far future under RCP4.5, unlike under RCP8.5, where increases are restricted only to Eastern Queensland.



226
227
228
229
230
231
232
233

Figure 6s. Future changes in solar power generation from mono-crystalline silicon cells. Panel a-f represents the future changes in solar power for ensemble members of CORDEX-Australasia for the near future (2030-2059) period under the RCP4.5 scenario. Panel g-l represents the future changes in solar power for ensemble members of CORDEX-Australasia for the far future (2070-2099) period under the RCP4.5 scenario.

Changes in Power Generation RCP8.5



234
235

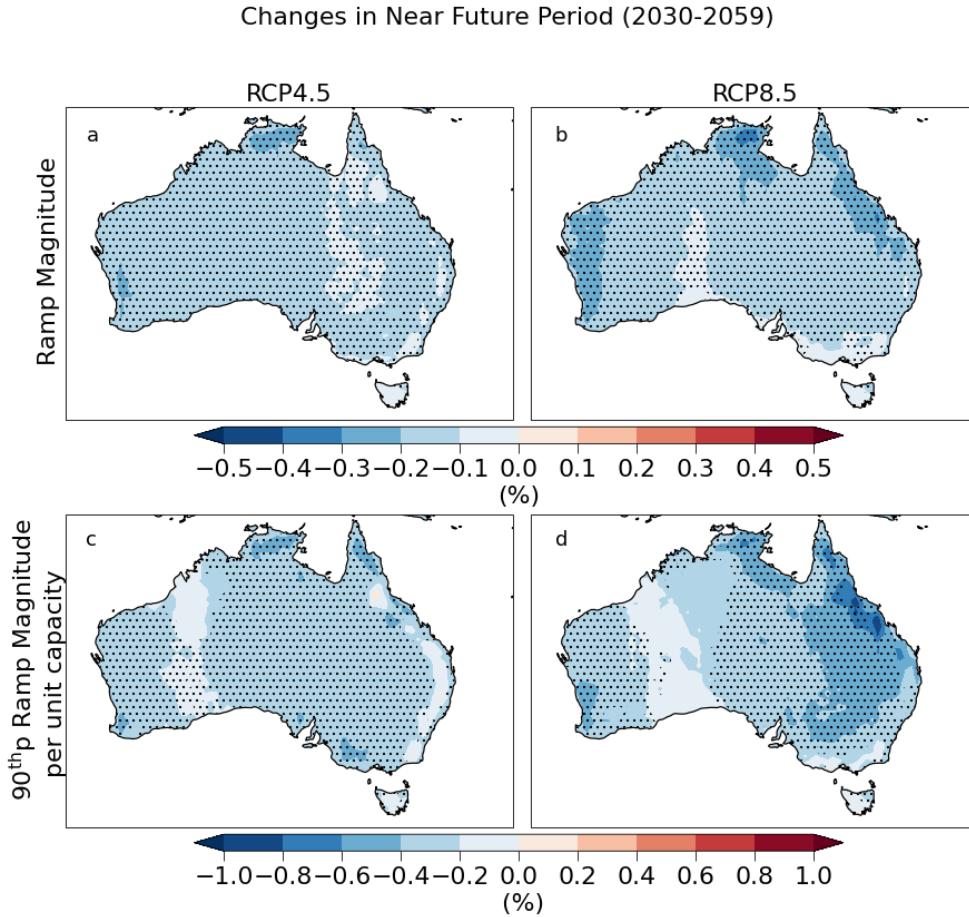
236 **Figure 7s.** Future changes in solar power generation from mono-crystalline silicon cells. Panel a-f
 237 represents the future changes in solar power for ensemble members of CORDEX-Australasia for the
 238 near future (2030-2059) period under the RCP8.5 scenario. Panel g-l represents the future changes in
 239 solar power for ensemble members of CORDEX-Australasia for the far future (2070-2099) period
 240 under the RCP8.5 scenario.

241
242
243
244
245
246
247
248
249
250
251
252
253
254
255
256
257
258

259
260
261
262
263
264

7. Near Future changes for the ramp characteristics across Australia under RCP4.5 and RCP8.5 scenario

Ramp Magnitude:



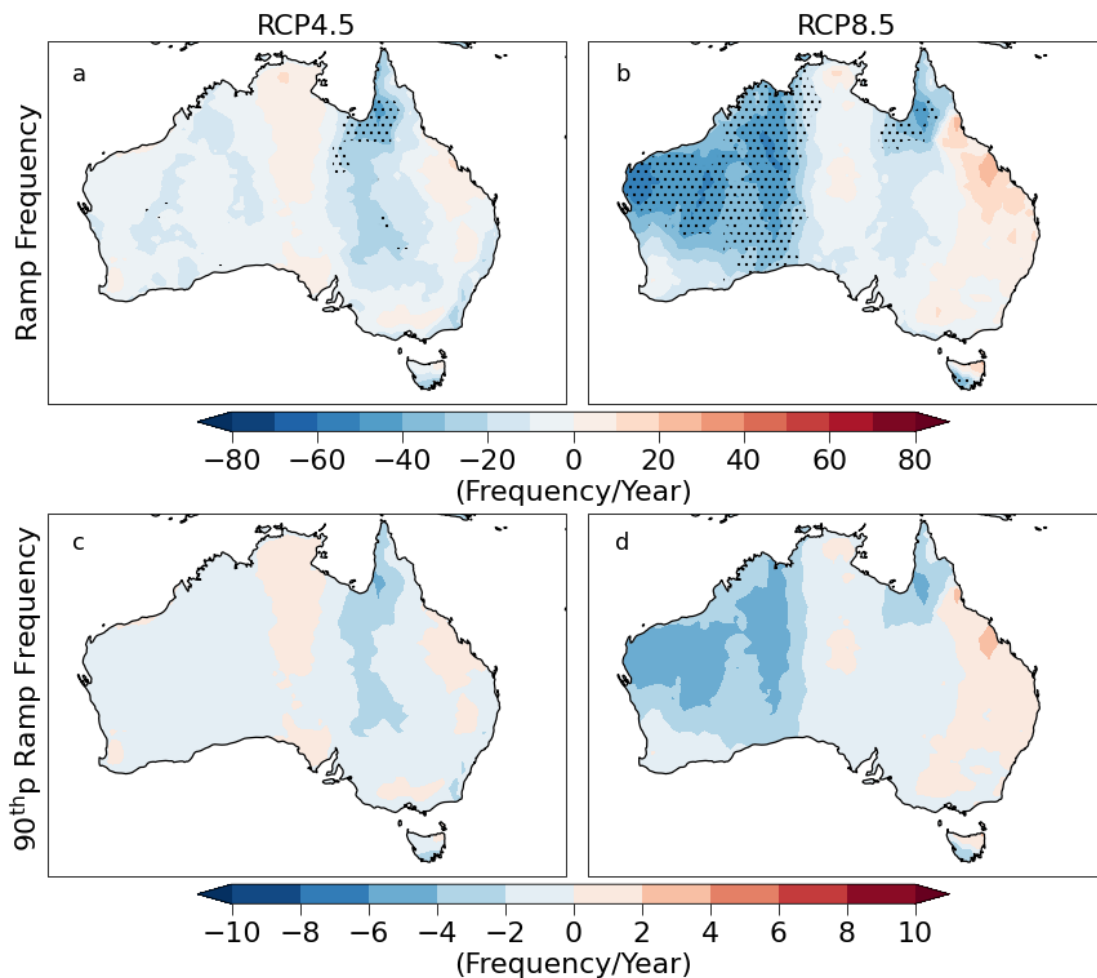
265
266
267
268
269
270
271
272
273
274
275
276
277
278
279

Figure 8s. Ramp magnitude change across Australia for the near future period (2030-2059). Panel a) and b) represent the future changes in mean ramp magnitude for the far future (2030-2059) period under RCP4.5 and RCP8.5. Panel c) and d) represent the future changes in ramp magnitude at the 90th percentile for the far future (2030-2059) period under RCP4.5 and RCP8.5. Stippling indicates a significant change (according to methods: significant test).

280

281 **Ramp Frequency:**

Changes in Near Future Period (2030-2059)



282

283 **Figure 9s.** Ramp frequency change across Australia for the near future period (2030-2099). Panel a)

284 and b) represent the future changes in mean ramp frequency per year for the near future (2030-2059)

285 period under RCP4.5 and RCP8.5. Panel c) and d) represent the future changes in the frequency of

286 ramps with ramp magnitude at the 90th percentile for the near future (2030-2059) period under

287 RCP4.5 and RCP8.5. Stippling indicates a significant change (according to methods: significant test).

288

289

290

291

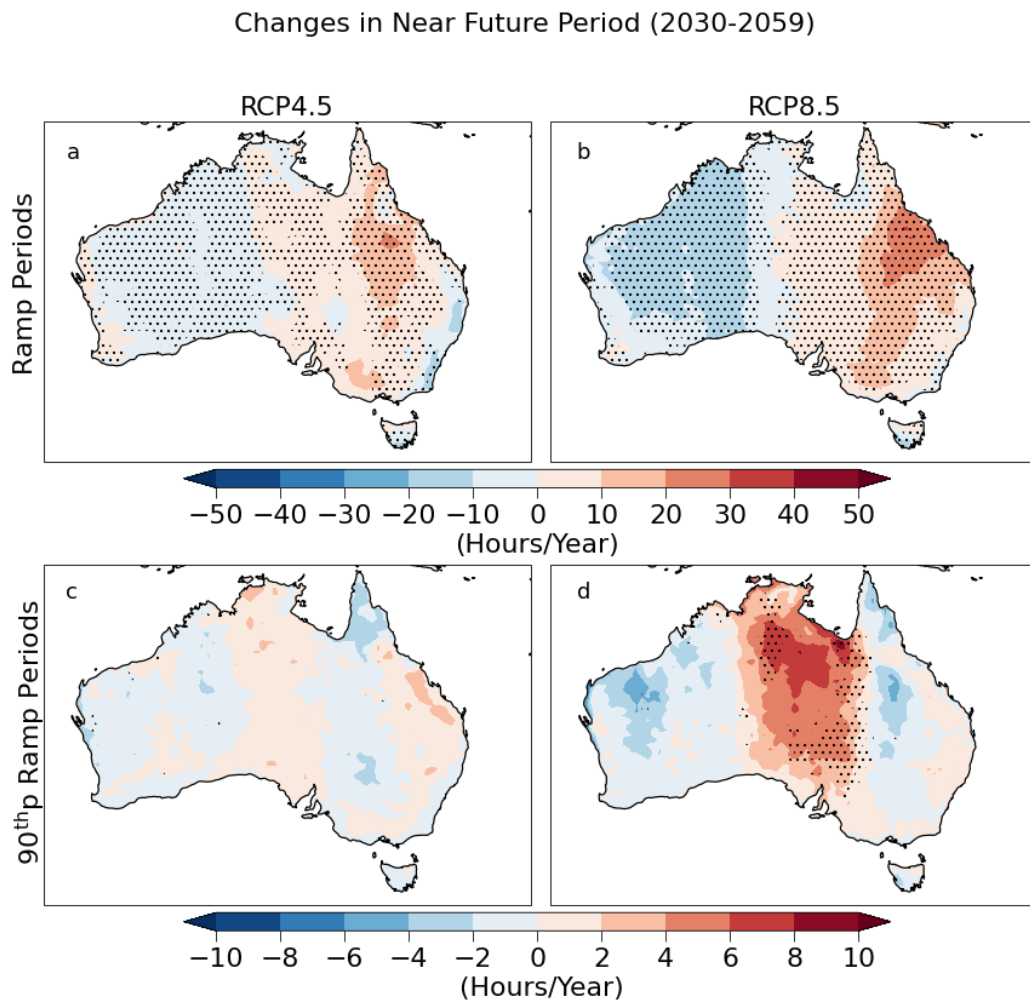
292

293

294

295 Ramp Periods:

296



297

298

299

300

301

302

303

304

305

306

307

308

309

310

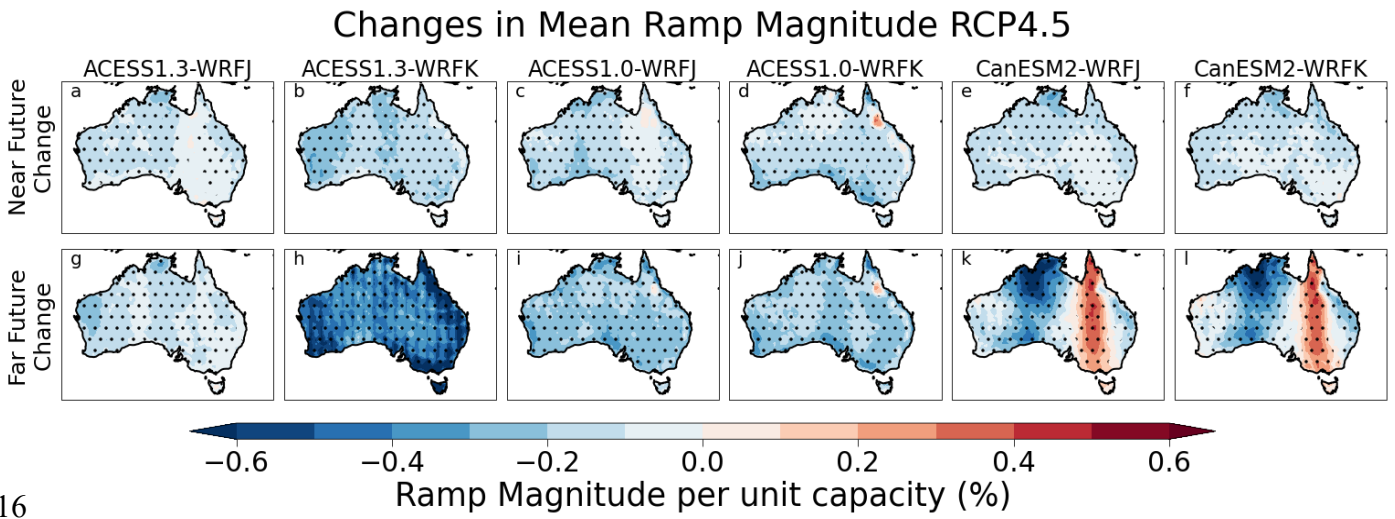
311

312

Figure 10s. Ramp period changes across Australia for the near future period (2030-2059). Panel a) and b) represent the future changes in mean ramp periods per year for the near future (2030-2059) period under RCP4.5 and RCP8.5. Panel c) and d) represent the future changes in ramp periods with ramp magnitude at the 90th percentile for the near future (2030-2059) period under RCP4.5 and RCP8.5. Stippling indicates a significant change (according to methods: significant test).

313
314
315

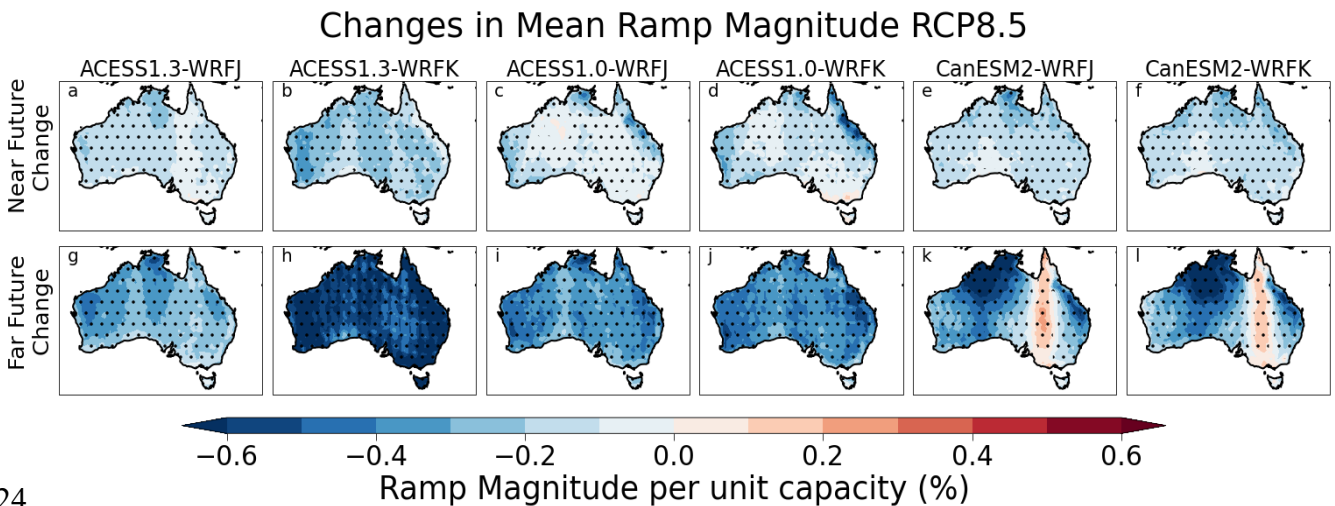
8. Future Changes in the mean ramp magnitude for each ensemble member under RCP4.5 and RCP8.5 scenario



316
317

318 *Figure 11s.* Future changes in mean solar power ramp magnitude. Panel a-f represents the future
319 changes in mean ramp magnitude for ensemble members of CORDEX-Australasia for the near future
320 (2030-2059) period under the RCP4.5 scenario. Panel g-l represents the future changes in mean
321 ramp magnitude for ensemble members of CORDEX-Australasia for the far future (2070-2099)
322 period under the RCP4.5 scenario.

323



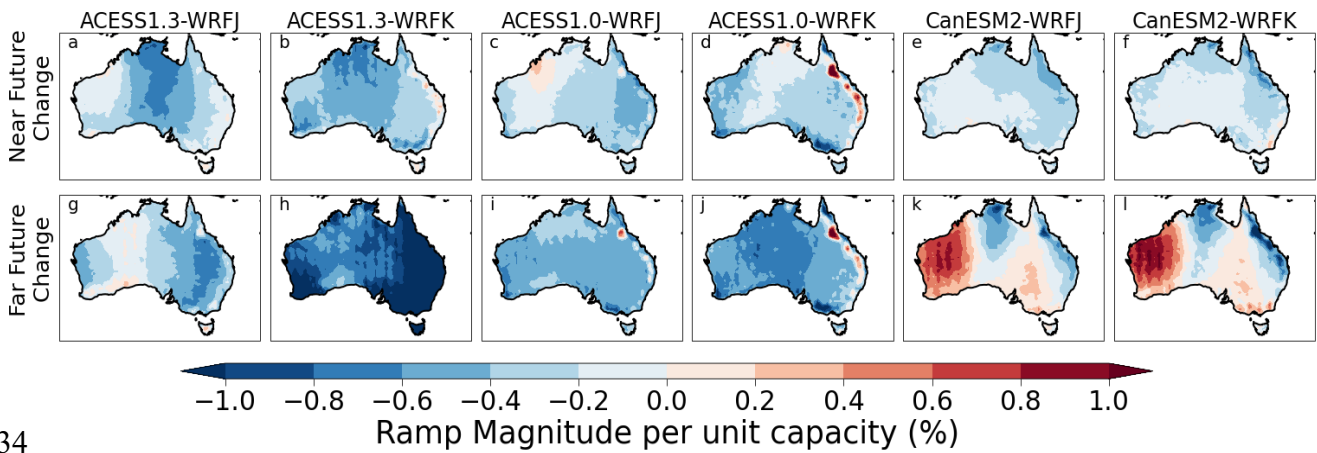
324
325

326 *Figure 12s.* Future changes in mean solar power ramp magnitude. Panel a-f represents the future
327 changes in mean ramp magnitude for ensemble members of CORDEX-Australasia for the near future
328 (2030-2059) period under the RCP4.5 scenario. Panel g-l represents the future changes in mean
329 ramp magnitude for ensemble members of CORDEX-Australasia for the far future (2070-2099)
330 period under the RCP4.5 scenario.

331

332 **9. Future Changes in the ramp magnitude at 90th percentile for each ensemble member**
 333 **under RCP4.5 and RCP8.5 scenario**

Changes in 90th Percentile Ramp Magnitude RCP4.5

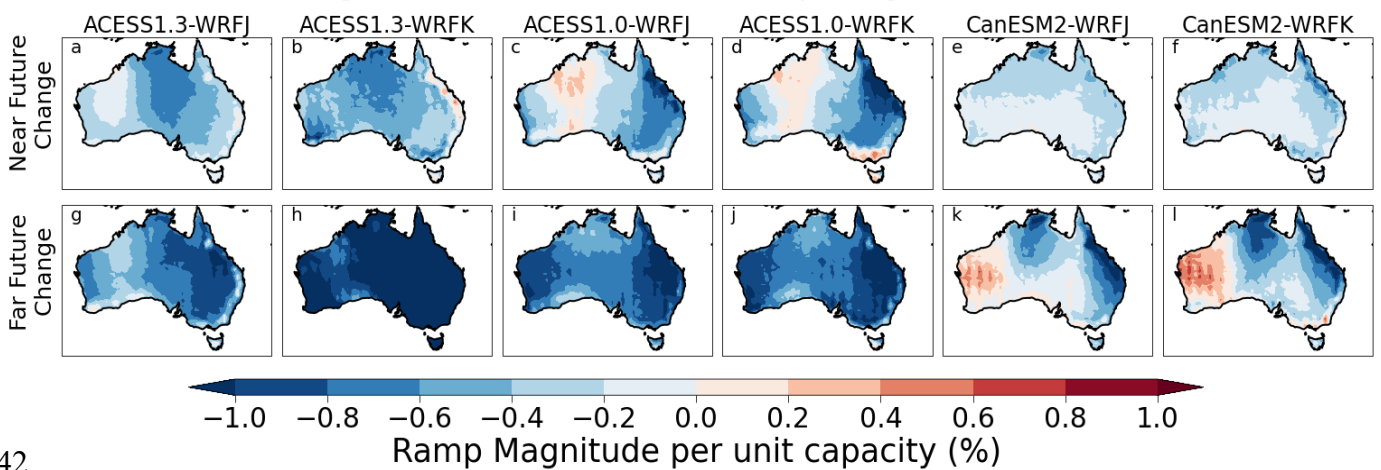


334
335

336 *Figure 13s. Future solar power ramp magnitude changes at the 90th percentile, representing extreme*
 337 *ramps. Panel a-f represents the future changes in extreme ramp magnitude for ensemble members of*
 338 *CORDEX-Australasia for the near future (2030-2059) period under the RCP4.5 scenario. Panel g-l*
 339 *represents the future changes in extreme ramp magnitude for ensemble members of CORDEX-*
 340 *Australasia for the far future (2070-2099) period under the RCP4.5 scenario.*

341

Changes in 90th Percentile Ramp Magnitude RCP8.5

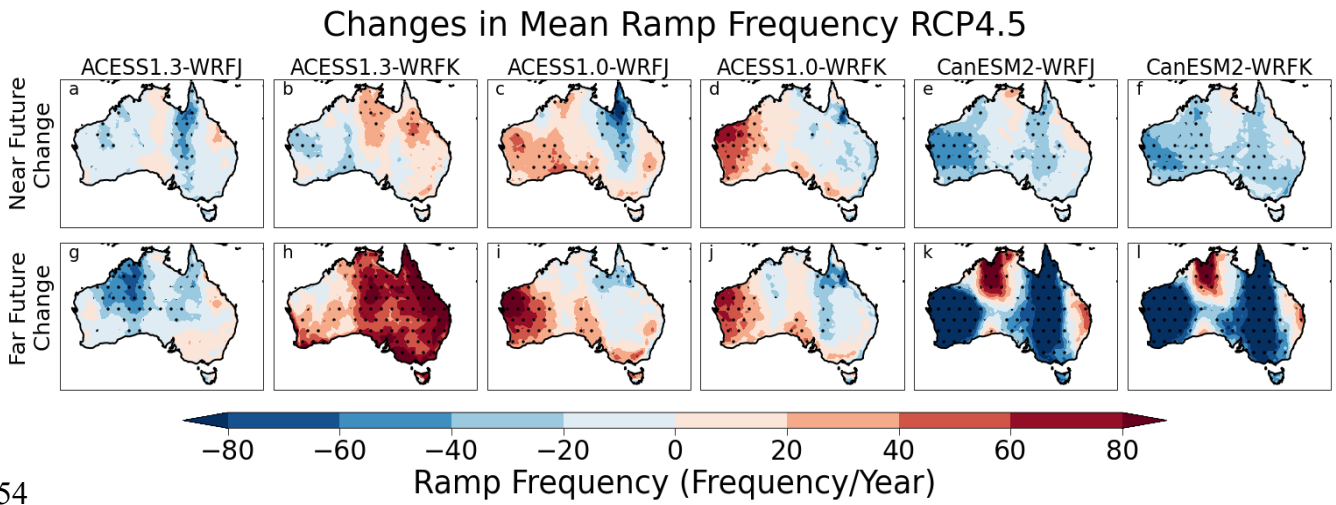


342
343

344 *Figure 14s. Future solar power ramp magnitude changes at the 90th percentile, representing extreme*
 345 *ramps. Panel a-f represents the future changes in extreme ramp magnitude for ensemble members of*
 346 *CORDEX-Australasia for the near future (2030-2059) period under the RCP8.5 scenario. Panel g-l*
 347 *represents the future changes in extreme ramp magnitude for ensemble members of CORDEX-*
 348 *Australasia for the far future (2070-2099) period under the RCP8.5 scenario.*

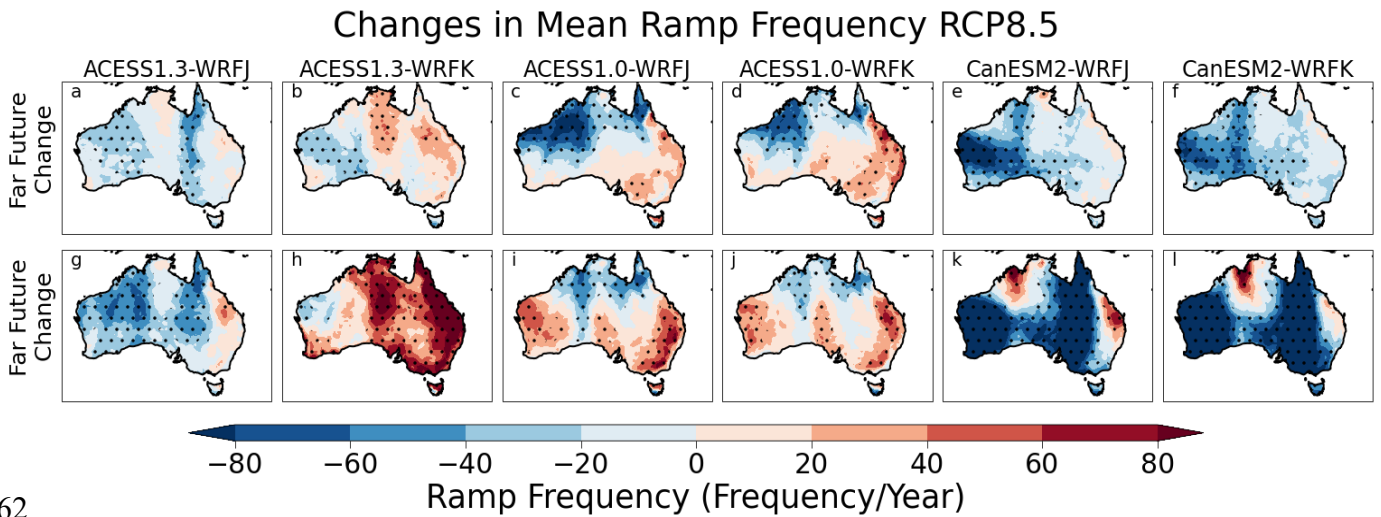
349

350 **10. Future Changes in the mean ramp frequency for each ensemble member under**
 351 **RCP4.5 and RCP8.5 scenario**
 352
 353



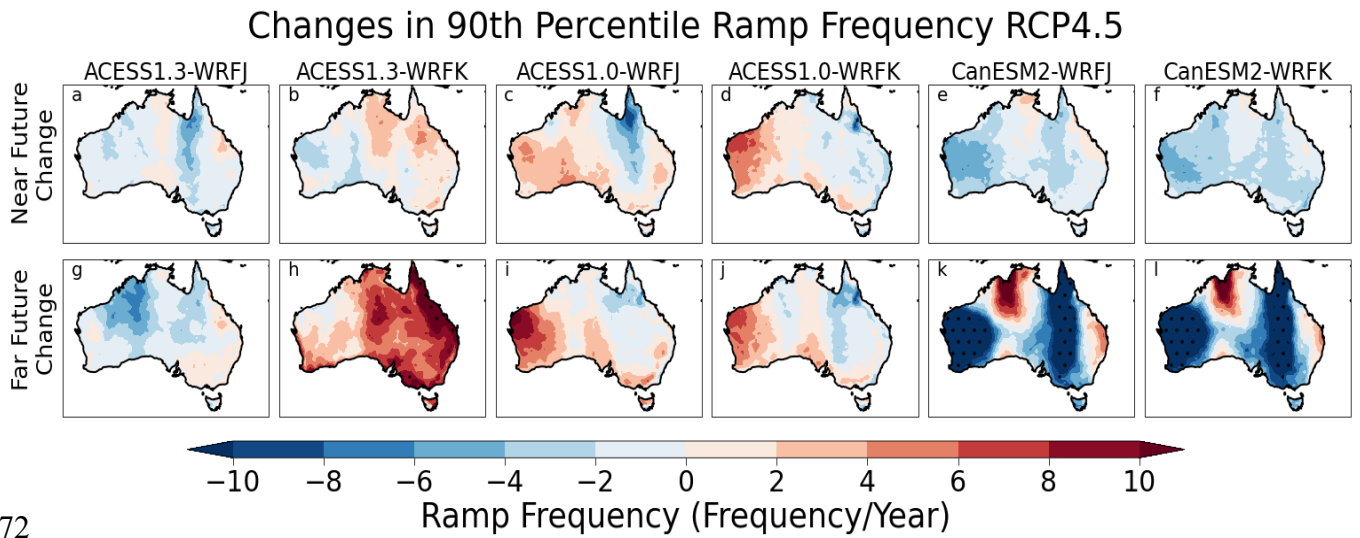
354
 355
 356 *Figure 15s. Future changes in mean solar power ramp frequency. Panel a-f represents the future*
 357 *changes in extreme ramp frequency for ensemble members of CORDEX-Australasia for the near*
 358 *future (2030-2059) period under the RCP4.5 scenario. Panel g-l represents the future changes in*
 359 *extreme ramp frequency for ensemble members of CORDEX-Australasia for the far future (2070-*
 360 *2099) period under the RCP4.5 scenario.*

361

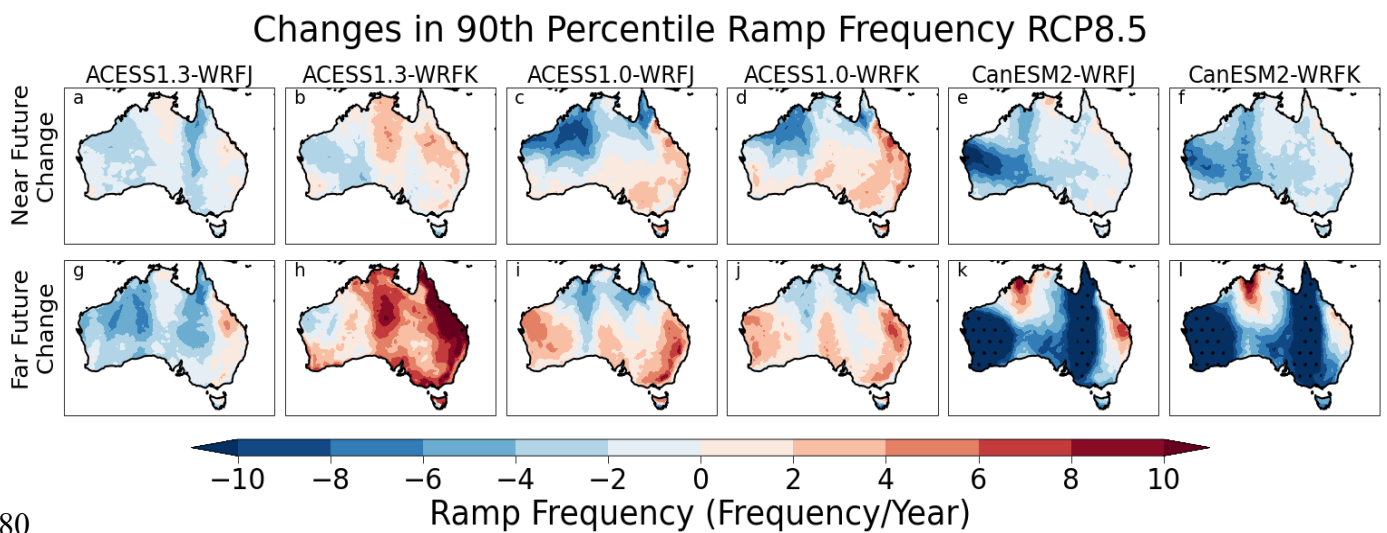


362
 363
 364 *Figure 16s. Future changes in mean solar power ramp frequency. Panel a-f represents the future*
 365 *changes in extreme ramp frequency for ensemble members of CORDEX-Australasia for the near*
 366 *future (2030-2059) period under the RCP8.5 scenario. Panel g-l represents the future changes in*
 367 *extreme ramp frequency for ensemble members of CORDEX-Australasia for the far future (2070-*
 368 *2099) period under the RCP8.5 scenario.*

369 **11. Future Changes in the frequency of ramp magnitude at the 90th percentile for each**
 370 **ensemble member under the RCP4.5 and RCP8.5 scenario**
 371



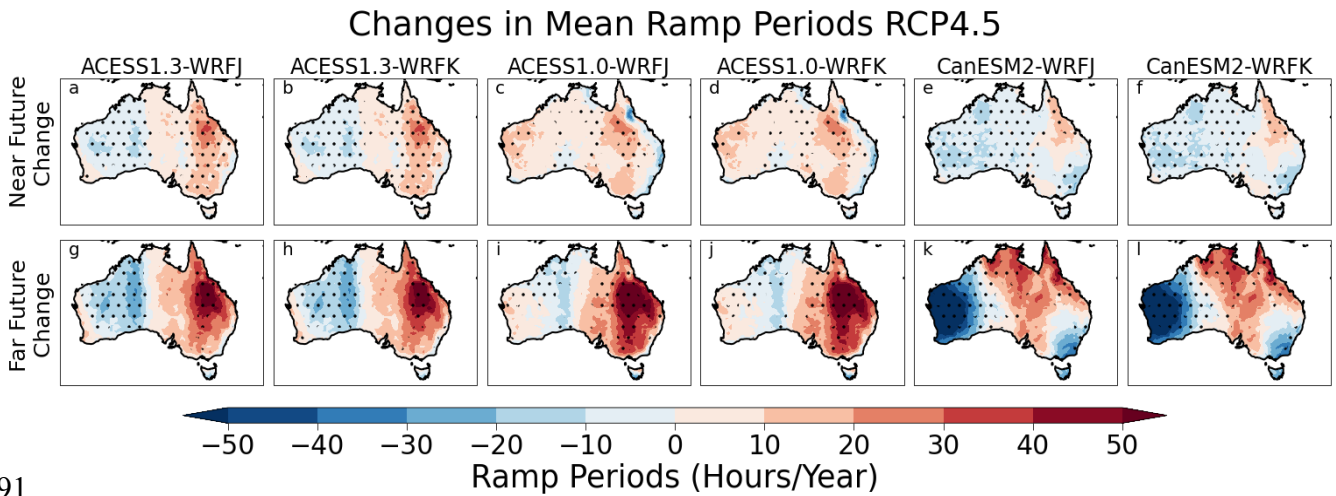
372
 373
 374 **Figure 17s.** Future changes in the frequency of ramps with ramp magnitude at the 90th percentile.
 375 Panel a-f represents the future changes in extreme ramp frequency for ensemble members of
 376 CORDEX-Australasia for the near future (2030-2059) period under the RCP4.5 scenario. Panel g-l
 377 represents the future changes in extreme ramp frequency for ensemble members of CORDEX-
 378 Australasia for the far future (2070-2099) period under the RCP4.5 scenario.
 379



380
 381
 382 **Figure 18s.** Future changes in the frequency of ramps with ramp magnitude at the 90th percentile.
 383 Panel a-f represents the future changes in extreme ramp frequency for ensemble members of
 384 CORDEX-Australasia for the near future (2030-2059) period under the RCP8.5 scenario. Panel g-l
 385 represents the future changes in extreme ramp frequency for ensemble members of CORDEX-
 386 Australasia for the far future (2070-2099) period under the RCP8.5 scenario.

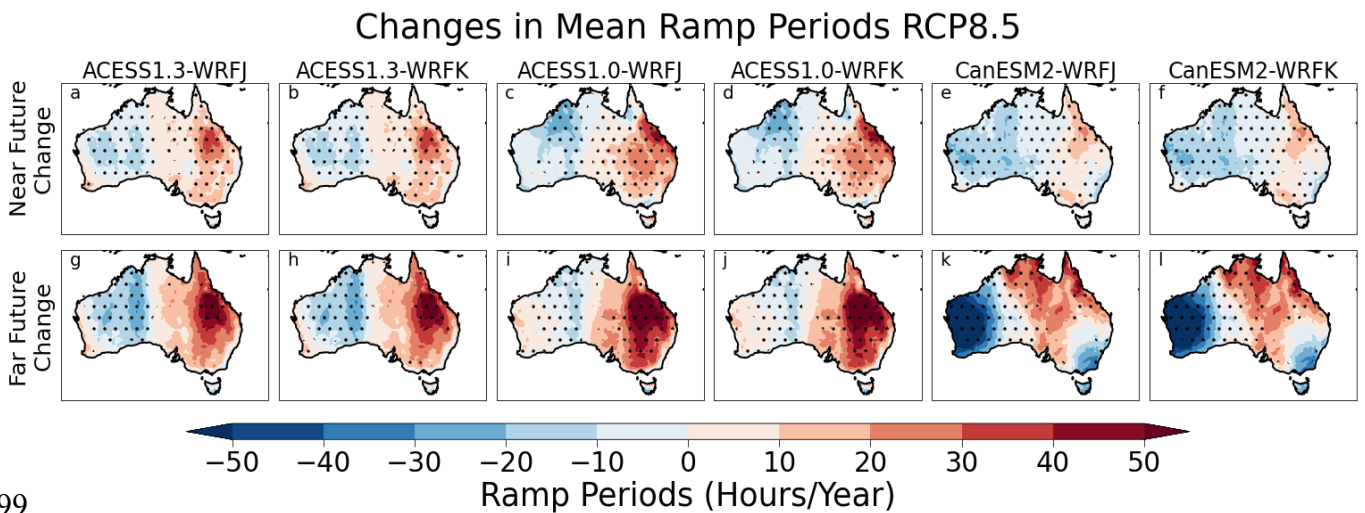
387 **12. Future Changes in the mean ramping periods for each ensemble member under**
 388 **RCP4.5 and RCP8.5 scenario**

389
 390



391
 392
 393
 394
 395
 396
 397
 398

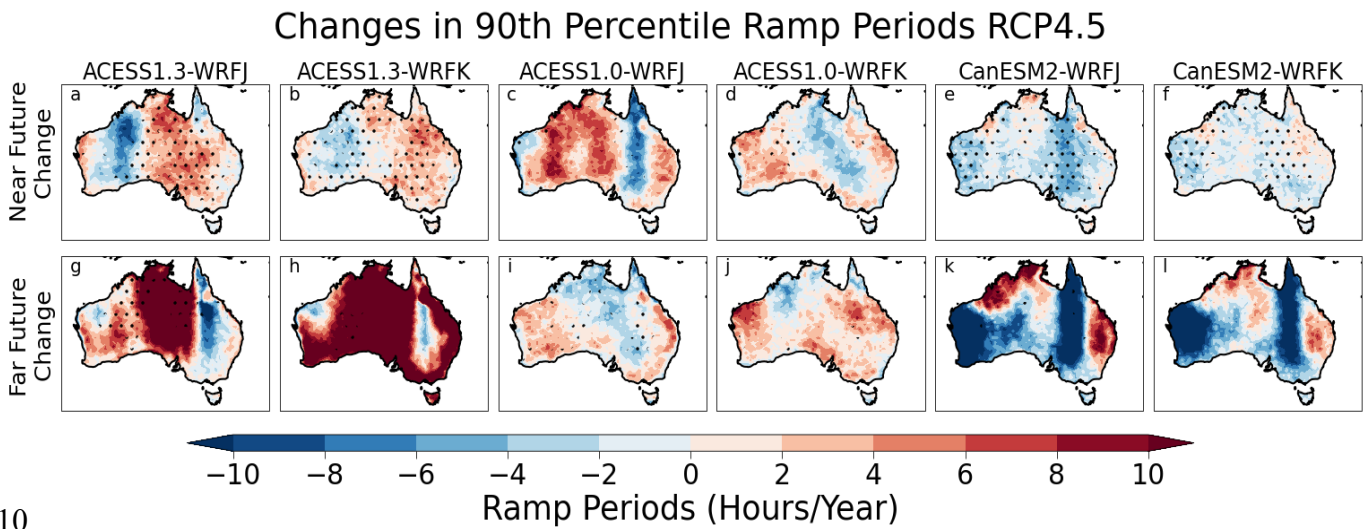
Figure 19s. Future changes in mean solar power ramping period. Panel a-f represents the future changes in mean ramp periods for ensemble members of CORDEX-Australasia for the near future (2030-2059) period under the RCP4.5 scenario. Panel g-l represents the future changes in the mean ramp period for ensemble members of CORDEX-Australasia for the far future (2070-2099) period under the RCP4.5 scenario.



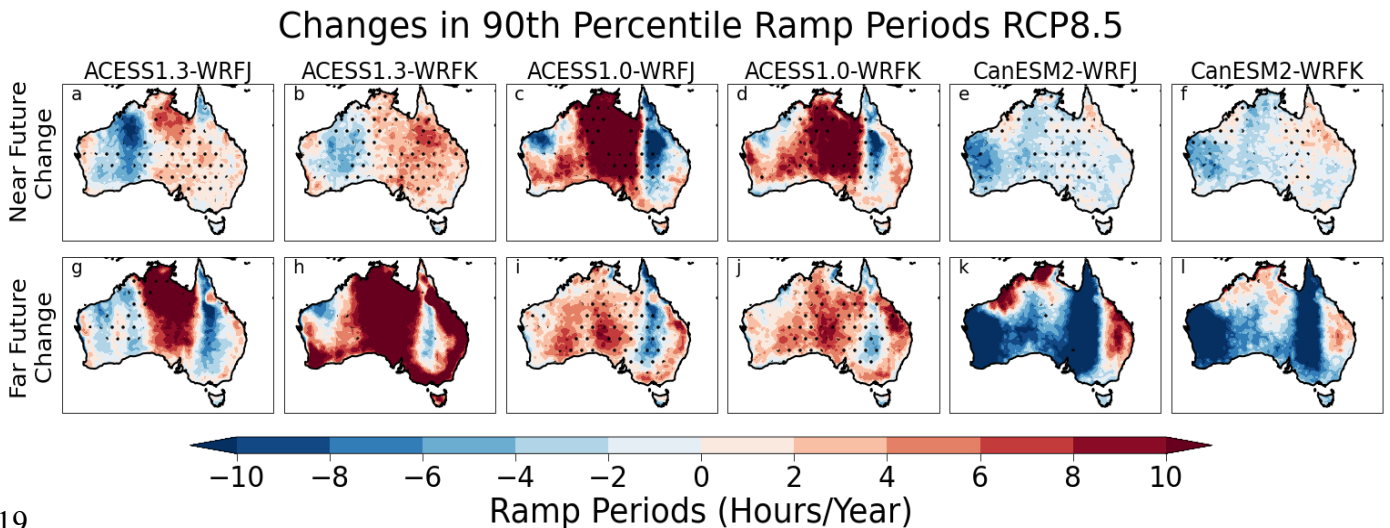
399
 400
 401
 402
 403
 404
 405

Figure 20s. Future changes in mean solar power ramping period. Panel a-f represents the future changes in mean ramp periods for ensemble members of CORDEX-Australasia for the near future (2030-2059) period under the RCP8.5 scenario. Panel g-l represents the future changes in the mean ramp period for ensemble members of CORDEX-Australasia for the far future (2070-2099) period under the RCP8.5 scenario.

406 **13. Future Changes in the ramping period of ramp magnitude at the 90th percentile for**
 407 **each ensemble member under the RCP4.5 and RCP8.5 scenario**
 408
 409



410
 411
 412 **Figure 21s.** Future changes represent the ramp periods with ramp magnitude at the 90th percentile.
 413 Panel a-f represents the future changes in the extreme ramp period for ensemble members of
 414 CORDEX-Australasia for the near future (2030-2059) period under the RCP4.5 scenario. Panel g-l
 415 represents the future changes in the extreme ramp period for ensemble members of CORDEX-
 416 Australasia for the far future (2070-2099) period under the RCP4.5 scenario.
 417
 418



419
 420 **Figure 22s.** Future changes represent the ramp periods with ramp magnitude at the 90th percentile.
 421 Panel a-f represents the future changes in the extreme ramp period for ensemble members of
 422 CORDEX-Australasia for the near future (2030-2059) period under the RCP8.5 scenario. Panel g-l
 423 represents the future changes in the extreme ramp period for ensemble members of CORDEX-
 424 Australasia for the far future (2070-2099) period under the RCP8.5 scenario.
 425

426

427 Reference:

428 [1] Reno MJ, Hansen CW. Identification of periods of clear sky irradiance in time series of GHI
429 measurements. *Renew Energy* 2016;90:520–31. <https://doi.org/10.1016/j.renene.2015.12.031>.

430